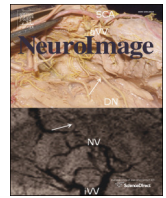




Contents lists available at ScienceDirect

NeuroImage

journal homepage: [www.elsevier.com/locate/ynimg](http://www.elsevier.com/locate/ynimg)

# Functional brain networks contributing to the Parieto-Frontal Integration Theory of Intelligence

Q1 Andrei A. Vakhtin<sup>b</sup>, Sephira G. Ryman<sup>b</sup>, Raneë A. Flores<sup>a</sup>, Rex E. Jung<sup>a,\*</sup>

4 <sup>a</sup> Department of Neurosurgery, University of New Mexico, Albuquerque, NM, USA

Q2 <sup>b</sup> Department of Psychology, University of New Mexico, Albuquerque, NM, USA

## ARTICLE INFO

### Article history:

8 Accepted 24 September 2014

9 Available online xxxx

### Keywords:

11 Intelligence

12 Reasoning

13 Networks

14 Independent component analysis (ICA)

15 Functional magnetic resonance imaging (fMRI)

## ABSTRACT

The refinement of localization of intelligence in the human brain is converging onto a distributed network that broadly conforms to the Parieto-Frontal Integration Theory (P-FIT). While this theory has received support in the neuroimaging literature, no functional magnetic resonance imaging study to date has conducted a whole-brain network-wise examination of the changes during engagement in tasks that are reliable measures of general intelligence (e.g., Raven's Progressive Matrices Test; RPM). Seventy-nine healthy subjects were scanned while solving RPM problems and during rest. Functional networks were extracted from the RPM and resting state data using Independent Component Analysis. Twenty-nine networks were identified, 26 of which were detected in both conditions. Fourteen networks were significantly correlated with the RPM task. The networks' spatial maps and functional connectivity measures at 3 frequency levels (low, medium, & high) were compared between the RPM and rest conditions. The regions involved in the networks that were found to be task related were consistent with the P-FIT, localizing to the bilateral medial frontal and parietal regions, right superior frontal lobule, and the right cingulate gyrus. Functional connectivity in multiple component pairs was differentially affected across all frequency levels during the RPM task. Our findings demonstrate that functional brain networks are more stable than previously thought, and maintain their general features across resting state and engagement in a complex cognitive task. The described spatial and functional connectivity alterations that such components undergo during fluid reasoning provide a network-wise framework of the P-FIT that can be valuable for further, network based, neuroimaging inquiries regarding the neural underpinnings of intelligence.

© 2014 Published by Elsevier Inc.

## Introduction

Modern neuroimaging techniques have allowed for increasingly fine-grained inquiries regarding the structural and functional brain correlates of human intelligence. Such techniques have evolved from early focus on discrete regional associations (Andreasen et al., 1993) to increasingly sophisticated inquiries that regard the brain as a network (van den Heuvel et al., 2009). While most early studies focused on the frontal lobes as the primary locus of human intelligence (Duncan et al., 2000; Gray et al., 2003), a review of structural and task-related functional neuroimaging literature suggested that the integrity of a distributed network involving the parietal and frontal regions best accounted for individual differences in intelligence (P-FIT; Jung and Haier, 2007). The theory has been supported by multiple brain lesion studies and analyses of healthy controls' cognitive data across different neuroimaging modalities (Colom et al., 2009; Deary et al., 2010; Gläscher et al., 2010; Li et al., 2009; Song et al., 2008). While the P-FIT

has received substantial attention from the intelligence community (Barbey et al., 2012; Deary, 2012; Langer et al., 2012; Luders et al., 2009), the broad nature of the theory's scope leaves much ambiguity for further investigations. This study thus aimed to test the P-FIT by isolating the specific functional brain networks that may contribute to it, and examine the changes such networks undergo in terms of their spatial distributions and inter-network connection strengths during a fluid reasoning task.

Our understanding of whole-brain processes has progressed substantially since the discovery of inter-hemispheric functional correlations in the motor cortex (Biswal et al., 1995). The existence of numerous functional brain networks, or brain regions that exhibit high degrees of intrinsic functional coherence, has since been confirmed using various approaches (Allen et al., 2012b). Analyses of such networks have demonstrated significant relationships between their various properties and cognitive functioning, providing a viable approach for investigating and detecting functional abnormalities in neurological and psychiatric disorders (Garrity et al., 2007; Jafri et al., 2008; Vakhtin et al., 2013). The network-wise approach produces readily interpretable results, and is a useful tool for establishing a framework for better understanding human cognition (Bressler and Menon, 2010).

\* Corresponding author at: 801 University Blvd. SE, Suite 202, Albuquerque, NM 87106, USA. Fax: +1 505 216 2623.

E-mail address: [rex.jung@gmail.com](mailto:rex.jung@gmail.com) (R.E. Jung).

Using independent component analysis (ICA; Bell and Sejnowski, 1995), the spatial distributions of resting state functional brain networks have been shown to be stable across multiple independent functional magnetic resonance imaging (fMRI) data sets, with their functions having been inferred using previously established roles of the involved anatomical regions (Allen et al., 2012a, 2012b). The spatial changes that such networks undergo as a response to cognitive engagement, however, have not been studied extensively. While maintaining their general features, multiple ICA-derived networks have previously been shown to alter their spatial distributions during an auditory oddball task (Calhoun et al., 2008). The robustness of such components during engagement in complex tasks, however, is yet to be investigated.

The Raven's Progressive Matrices Test (RPM; Raven, 2000) has been determined to be one of the best tools for measuring fluid reasoning ability, which in turn is highly related to general intelligence (Snou et al., 1984). The task is based on visual stimuli, overcoming the challenges presented by using verbally mediated tasks to measure intelligence in multicultural samples. Previous neuroimaging studies have revealed that fluid cognitive processes induced by RPM activate areas consistent with the P-FIT, localizing to the bilateral frontal and parietal regions (Duncan et al., 2000; Haier et al., 1988; Kroger et al., 2002; Prabhakaran et al., 1997). We therefore considered the RPM task as a suitable candidate for inducing activity within the functional brain networks that contribute to general intelligence and comparing them to their resting states. Since the performance on measures that assess fluid reasoning (e.g., Ravens Progressive Matrices) represents relatively complex cognitive processes, we hypothesized that widespread spatial redistributions of functional networks would be observed during fluid reasoning when compared to during rest.

Given the widespread spatial effects that cognitive load is able to induce in functional brain networks, we expected parallel changes in levels of functional network connectivity (FNC) between different pairs of networks. While parieto-frontal connectivity has been associated with higher levels of intelligence in both adults and children (Langeslag et al., 2013; Song et al., 2008), the specific networks involved have not been identified. Importantly, we hypothesized that such changes in FNC between rest and fluid reasoning tasks would not be consistent across different frequencies of the networks' time courses. While it has been shown that functional brain networks primarily exhibit low frequency oscillations and tend to rely on these frequencies in their connections to each other (Cordes et al., 2000), such effects appear to be predominant in sensorimotor, visual, language, and auditory networks. Since such networks are of little interest in our goal of investigating complex cognitive processes involved in fluid reasoning, we hypothesized that FNC in cognitive, default-mode (DMN), and attention networks may not be limited to these low frequencies during complex cognitive tasks. Functional connectivity changes evoked by fluid reasoning were therefore explored across the full spectrum by examining low, medium, and high frequency bands. The main purpose of the FNC analysis was to isolate the networks and frequencies that contribute to the integration of the frontal and parietal regions, which would subsequently be used as stepping stones to investigate their relationships with individual differences in fluid reasoning ability.

## 130 Methods

131 Seventy-nine subjects (46 males,  $21.7 \pm 3.1$  years old) were recruited for the study from the University of New Mexico (UNM), Albuquerque, NM, USA. Prior to study enrollment, each participant signed a consent form explaining the procedures and their potential risks. 132  
133 The study and consent form were approved by the UNM Institutional Review Board. All subjects were screened for and excluded if they 134  
135 reported any past major head injuries, psychiatric or neurological 136  
137 disorders, substance abuse, and intake of any psychoactive medications. 138

The fMRI data were collected using a 3-T Siemens Trio scanner at the 139  
Mind Research Network (MRN), Albuquerque, NM. Each participant 140  
went through 3 sessions in the scanner: a resting state scan and 2 141  
sessions while solving problems from the Standard and Advanced 142  
Raven's Progressive Matrices Test (Raven, 1990). Ten matrices were 143  
pseudorandomly sampled from six versions of the test, including all 144  
difficulty levels of the items, for each RPM session. The RPM sessions 145  
consisted of 10 problems each, with each matrix presented at the center 146  
of the screen and four possible answer choices below. Subjects made 147  
selections by pressing one of four buttons corresponding to the index 148  
and middle finger of both hands. Each problem was presented for 149  
15 s, with a standard 15-second interstimulus interval maintained 150  
throughout each block, during which a cross hair was presented. All 151  
participants went through 2 training sessions on the RPM task before 152  
their fMRI scans, with none of the problems being presented more 153  
than once. During the resting state scan, participants were instructed 154  
to stare at a fixation cross presented on the screen in front of them, 155  
relax, and think of nothing in particular. 156

The T2\*-weighted functional images were collected using a 157  
gradient-echo echo planar imaging sequence with an echo time of 158  
29 ms, repetition time of 2 s, flip angle of 75°, slice thickness of 159  
3.5 mm, distance factor of 30%, field of view of 240 mm, matrix size 160  
of  $64 \times 64$  voxels, and voxel size of  $3.8 \text{ mm} \times 3.8 \text{ mm} \times 3.5 \text{ mm}$ . 161  
A total of 5 min, 16 s of resting state data were collected, while 162  
each RPM scan lasted 5 min and 50 s. The resulting data were slice 163  
timing-corrected and smoothed with a 10 mm kernel using the 164  
automated neuroimaging pipeline set up at MRN, which is described 165  
in further detail elsewhere (Bockholt et al., 2010; Scott et al., 2011). 166  
Data from subjects who moved more than 3.5 mm during any single 167  
inter-scan period were excluded from further analyses. 168

Spatial independent component analysis was used to examine the 169  
temporal correlations in signal fluctuations between multiple brain 170  
regions, producing a set of independent components with high intrinsic 171  
temporal coherences that were maximally independent in space. The 172  
algorithm utilizes blind source separation to reduce the data to a 173  
number of components specified by the user. Its data-driven nature 174  
makes it applicable to resting state scans, which do not possess any temporal 175  
information necessary for conventional fMRI analyses. We used 176  
the Group ICA of fMRI Toolbox (GIFT; <http://mialab.mrn.org/software>) 177  
to separately extract 75 components from the resting state and task 178  
sessions, producing a whole-head spatial t-map and a signal time course 179  
for each one. Non-artifactual functional brain networks were then selected 180  
from the resulting data sets according to previously identified 181  
components (Allen et al., 2011; Smith et al., 2009), and all further 182  
analyses were concerned solely with such networks. Spatial cross- 183  
correlations of networks were performed between resting and RPM 184  
sessions in order to detect networks present in both conditions, 185  
deeming a network stable if its Pearson's  $r$  was greater or equal to 0.5. 186

Using the Statistical Parametric Toolbox 8 (SPM8), a unique behavioral 187  
block design was created for each subject and RPM session, 188  
modeling the time interval during which the problem was presented 189  
on the screen. The model was convolved with the canonical hemodynamic 190  
response function, and all the subjects' data were horizontally 191  
concatenated within each session. Likewise, each network's time 192  
course was horizontally concatenated across subjects in each session, 193  
and the two variables were entered into a regression analysis 194  
for all networks in every RPM session. Components were classified 195  
as task related if their time courses were significantly correlated 196  
with the behavioral model ( $FDR p = 0.001$ ). 197

All networks' whole-head spatial maps from each session (rest, 198  
RPM1, and RPM2) were z-scaled and entered into a within-subject 199  
ANOVA to investigate the effects of RPM task on networks' spatial 200  
distributions. A spatial mask was used in the analysis, and was 201  
obtained by entering all 3 sessions' data from each network into a 202  
1 sample  $t$  test and applying an FDR-corrected threshold of  $p = 1e-10$  203  
to the results. 204

Functional connectivity was examined in all possible pairs of functional networks. Three band-pass filters were first applied to each network's time course, producing low (0.01–0.083 Hz), medium (0.084–0.166 Hz), and high (0.167–0.25 Hz) frequency datasets. We utilized the Functional Connectivity Toolbox (<http://mialab.mrn.org/software>) to obtain a correlation coefficient for each network pair's low, medium, and high frequency connectivity in every session and subject. For every network pair, the correlation coefficients were Fisher z-transformed and entered into a mixed linear model with session (rest, RPM1, RPM2) and frequency (low, medium, high) as fixed factors and subjects as random factors.

## Results

The subjects averaged accuracy rates of  $.68 \pm .02$  and  $0.57 \pm .02$  on the first and second RPM sessions, respectively. A subsequent paired *t* test revealed the difference in performance between the RPM sessions to be significant ( $t(78) = 5.41, p < 0.001$ ). Since the difficulty levels of the RPM problem sets were the same, this effect is likely attributable to fatigue over successive sessions. Since we were not concerned with performance-correlated brain activity in this study, however, we did not account for this effect in the subsequent analyses of individual networks.

Twenty-nine functional brain networks were identified in the set of 75 independent components produced by GIFT (Fig. 1), and were subsequently classified according to function using previous ICA literature on the anatomical regions involved. The networks included attentional (A1–A6), cognitive (C1–C6), default-mode (D1–D3), sensorimotor (S1–S6), visual (V1–V6), auditory (AU), and basal ganglia (BG). Cross-correlations of the network spatial maps between resting state and RPM sessions revealed that 26 of the networks were present during both conditions. One sensorimotor network that was

detected during rest was not identified during task performance. Likewise, 2 cognitive networks were active only during the task, but not rest. Ten networks' time courses were significantly correlated with their respective behavioral models and thus classified as task-related (FDR  $p = 0.001$ ).

The analysis of networks' spatial distributions revealed significant effects of task in contrast to resting state in multiple components, both related and unrelated to the RPM task. These spatial effects are presented in Fig. 1 along with the networks' distributions in each condition. The specific regions involved can be found in the Supplementary material. The functional connectivity analysis revealed significant interactions of session and frequency in 14 task-related network pairs (Fig. 2). The interactions were examined in terms of simple effects of session on functional connectivity within each frequency band. The results indicated that increases in FNC during fluid reasoning varied across frequencies in different component pairs (Fig. 3). Additional main effects of session were detected in 5 pairs of networks, 3 of which were positive (Fig. 3). The integration of 2 interconnected network systems appeared to be activated by the RPM task: V2–A1–A3–D1 and V2–C2–A2–V1.

## Discussion

This is the first fMRI study to contrast networks' spatial distributions and functional connectivity data collected during resting state and engagement in Raven's Progressive Matrices test, a classic measure of general intelligence. We found a discrete set of networks to be associated with fluid reasoning, which largely overlapped regions first identified in the Parieto-Frontal Integration Theory, including the dorsolateral prefrontal cortex, inferior and superior parietal lobule, anterior cingulate, and regions within the temporal and occipital lobes. One of the main weaknesses of the original theory, that it did not explicitly address the network characteristics of the numerous

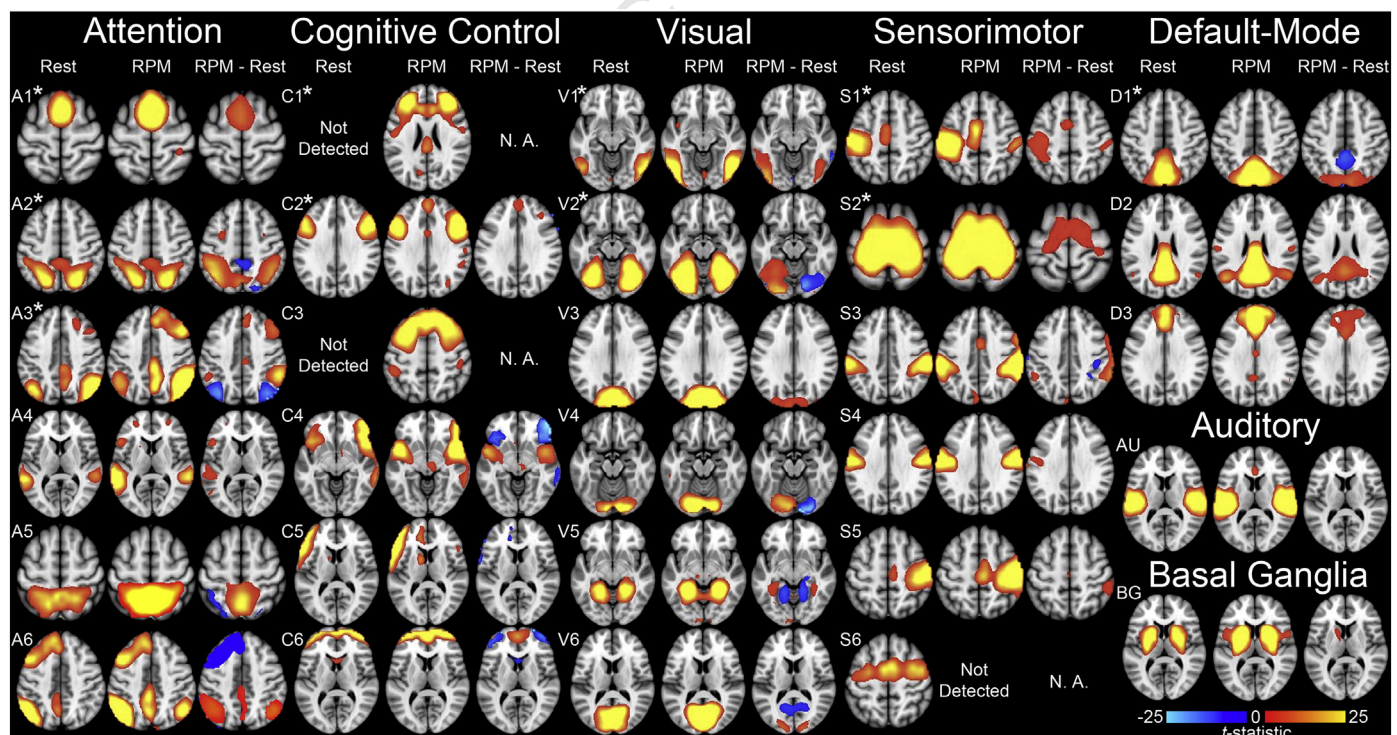


**Fig. 1.** Twenty-nine networks were identified: 6 attentional (A1–A6), 6 cognitive control (C1–C6), 6 visual (V1–V6), 6 sensorimotor (S1–S6), 3 default-mode (D1–D3), auditory (AU), and the basal ganglia (BG). Twenty-six of the networks were detected in both resting state and Raven's Progressive Matrices Test (RPM) conditions. The networks' spatial distributions during rest and performance of Raven's Progressive Matrices task (RPM) are plotted as 1 sample *t* test statistics on standard-space Montreal Neurological Institute 152 volumes, with warm colors representing intrinsic network coherence values. The RPM–rest contrasts are presented for each network as well, with warm and cool colors marking areas of significant increases and decreases, respectively, in intrinsic network coherences during the RPM task, as revealed by the repeated measures ANOVA (FDR  $p = 0.001$ ). Networks were functionally classified and ranked according to their degrees of task-relatedness. (\*) denotes networks that were significantly related to the RPM task (FDR  $p = 0.001$ ).

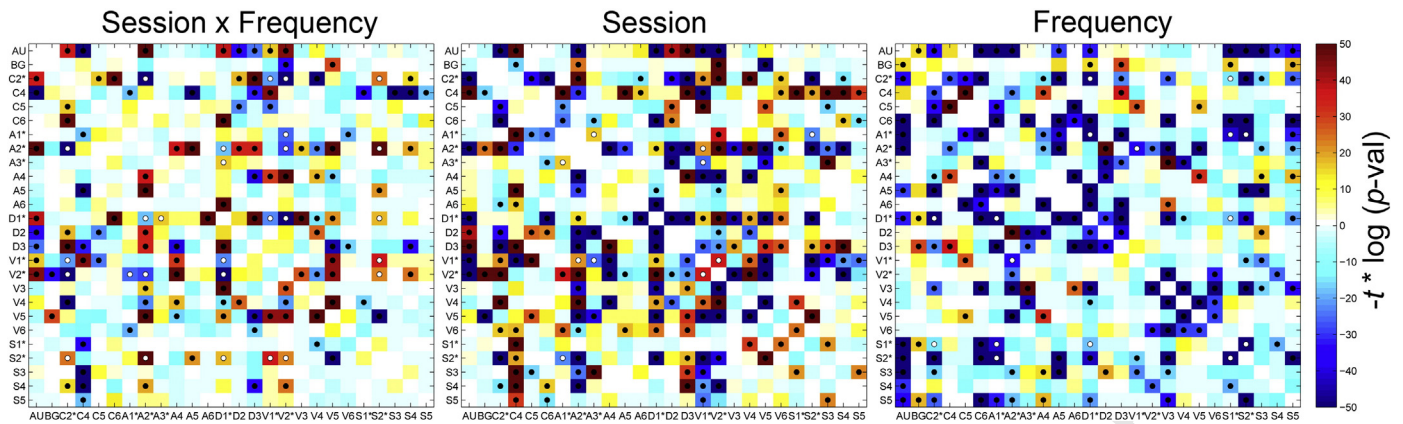


**Fig. 2.** Functional network connectivity results. The session  $\times$  frequency interaction (left) was significant in 14 pairs of networks (FDR  $p = 0.001$ ), which are marked by a white dot. Session effects (middle) were detected in 5 pairs of networks (FDR  $p = 0.001$ ), with each significant bin in which an interaction was not observed marked by a white dot. Frequency effects (right) were found in 8 pairs (FDR  $p = 0.001$ ), with the white dots marking those in which the interaction was not significant. (\*) indicates that the network was significantly related to the task.

regions identified, is now addressed using ICA, supporting underlying network characteristics of brain organization involved in fluid reasoning ability. While attention and cognitive networks were found to be task related, we also found several sensorimotor, visual, and a DMN to be significantly related to the RPM task. Interestingly, all frequency bands (low, medium, and high) were represented in significant functional connectivity interactions, with two distinct network systems being activated by the RPM task: visual-attention-DMN and visual-cognitive-attention.

Most of the functional networks derived from the resting state data were also present during the RPM task, with 26 networks being detected in both conditions. Such networks exhibited high degrees of spatial correlations between resting state and RPM scans, yet demonstrated significant levels of plasticity in their distributions, as seen in the spatial results. These networks are thus able to alter their activity levels and spatial distributions, while preserving their general spatial features even during complex problem solving. Oddly, one of the networks

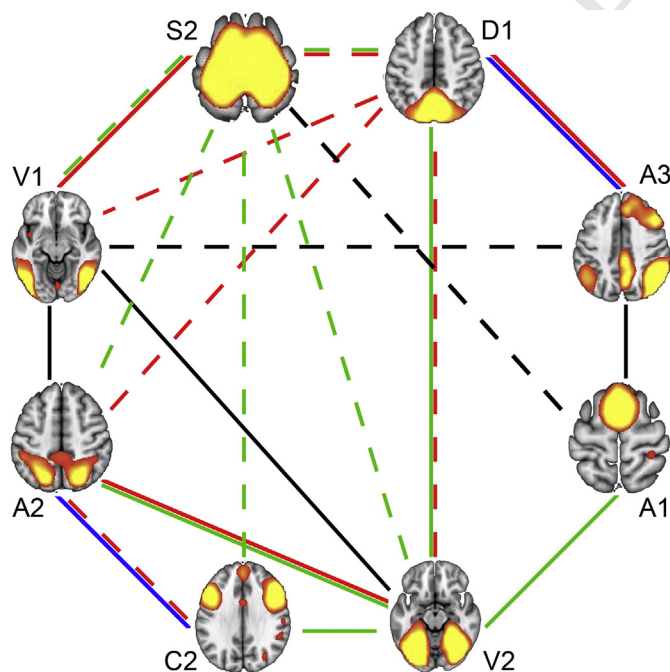


**Fig. 3.** Functional network connectivity differences induced by the RPM task. Solid lines represent increases in FNC, while the dashed lines represent FNC decreases as networks switch from resting state to performing the task. The frequencies in which such differences were observed are represented by the colors red (high), blue (medium), and green (low).

observed only during rest was classified as a sensorimotor component. Given component S6's spatial distribution and low relatedness to the task, we speculate that the network may be responsible for sensory processes, explaining the network's activity during the resting state scan, often associated with self-referential thoughts, but not while focusing on the RPM task.

The C1 component, on the other hand, was significantly related to the task and detected during the RPM task, but not during rest. Given that the component's main functional regions included the bilateral medial frontal and superior temporal gyri, it appears to be consistent with the frontal and temporal regions proposed by the P-FIT to modulate performance on intelligence measures. In addition, the superior temporal gyri have been implicated to play a role in integration of previous task actions and outcomes with future decision-making strategies (Paulus et al., 2005). An important limitation to our inferences about the networks that were not detected in both conditions is that their responses to cognitive load in comparison to rest could not be determined. Although the C1 network had the highest degree of task relatedness, we were not able to include it in the spatial or FNC analyses. Further investigations of the C1 network should be undertaken in order to establish the extent to which, if any, its coherence during fluid reasoning may be correlated with other aptitudes. We note that the C3 network was also specific to the RPM condition, but not necessarily of interest to this study due to the fact that it was not significantly related to the task.

While the task related networks exhibited the most widespread changes in their spatial distributions during the RPM task, multiple other networks were affected by the RPM task to some degree. In fact, the auditory network was the only one in which no spatial effects were detected. The widespread effects of a complex task like RPM were expected, and the functional classification of ICA-derived networks and their task relatedness measures aided us in focusing on the components relevant to fluid reasoning.

The regions involved in the networks that were found to be task related were broadly consistent with the P-FIT. Task related attentional networks localized to the bilateral medial frontal and parietal regions, right superior frontal lobule, and the right cingulate gyrus. Cognitive network C2 involves the right and left lateral frontal regions, which have previously been shown to be involved in decision-making processes (Duncan and Owen, 2000). Two sensorimotor networks were task-related, with the left motor strip being the main contributor to the S1 component, likely due to the subjects' use of the right hand when indicating responses to problems. Two visual networks were related to the task, and were localized to the bilateral occipital gyri. Finally, only one DMN was significantly related to the RPM task, spanning the bilateral precuneus. Interestingly, the precuneus has been associated

with visualization and imagination ability (Hassabis et al., 2007), likely important to visuo-spatial processing demands of the RPM task.

The functional connectivity analysis between task related networks revealed that the components utilize a broad range of frequencies in their integration during cognitive load, with significant positive and negative changes observed in low, medium, and high frequencies. Additionally, the V2 network emerged as a hub between two distinct clusters of networks that exhibited increases in FNC: V2–A1–A3–D1 and V2–C2–A2–V1. Given that the cognitive frontal network C2 is in the latter cluster, we speculate that it may be the network group responsible for the decision-making processes during fluid reasoning. Further analyses could investigate the relationship between variables of interest such as IQ and the FNC changes that network pairs undergo when switching from resting state to fluid reasoning.

There are several weaknesses associated with our approach. First, the use of the RPM could be interpreted to bias the functional networks towards fronto-parietal regions. However, the RPM is considered to be the best measures of fluid reasoning ability in the psychometric literature, and is highly correlated with other measures of intelligence (Raven, 2000), thus making it a good proxy measure of the cognitive construct of interest (i.e., “intelligence”). Our sample consisted of young, healthy, college students who were likely of higher intellectual capacity than average. Thus, the generalizability of the current results to populations that are older, include patients with neurological and psychiatric disorders, and who are of average or lower intellectual capacity is unknown. Finally, the use of ICA might be construed as artificially segmenting brain regions into maximally independent networks. Two main assumptions are made with ICA: that the sources are independent and that the distributions are non-Gaussian. Either or both of these might be violated with respect to functional brain imaging data. We make note that other techniques that do not rely on maximal separation of structural or functional brain regions have found a high correspondence between measures of intelligence and those identified with the P-FIT. Future studies utilizing other measures of “intelligence” (e.g., Wechsler Scales, “g”), more diverse samples (e.g., younger/older, broader IQ range), and other sophisticated analyses (e.g., graph theory) will help to determine the veracity of our findings over time.

The findings described in this paper provide a network-wise framework for targeting future neuroimaging analyses focusing on fluid reasoning and general intelligence (i.e., “g”). We have isolated the functional brain networks that are related to fluid reasoning, which correspond to the model of intelligence proposed by the P-FIT. The described spatial and FNC contrasts between fluid reasoning and rest provide further insight into the network-wise P-FIT framework, allowing for targeted examinations of aptitude correlates with brain function in future studies.

## Acknowledgments

This research was supported by a grant from the John Templeton Foundation entitled “The Neuroscience of Scientific Creativity.”

## Conflict of interest

The authors have no conflicts to disclose.

## Appendix A. Supplementary material

Supplementary data to this article can be found online at <http://dx.doi.org/10.1016/j.neuroimage.2014.09.055>.

## References

Allen, E.A., Erhardt, E.B., Damaraju, E., Gruner, W., Segall, J.M., Silva, R.F., Havlicek, M., Rachakonda, S., Fries, J., Kalyanam, R., Michael, A.M., Caprihan, A., Turner, J.A.,

Eichele, T., Adelsheim, S., Bryan, A.D., Bustillo, J., Clark, V.P., Feldstein Ewing, S.W., Filbey, F., Ford, C.C., Hutchison, K., Jung, R.E., Kiehl, K.A., Koditwakkhu, P., Komesu, Y.M., Mayer, A.R., Pearlson, G.D., Phillips, J.P., Sadek, J.R., Stevens, M., Teuscher, U., Thoma, R.J., Calhoun, V.D., 2011. A baseline for the multivariate comparison of resting-state networks. *Front. Syst. Neurosci.* 5, 2.

Allen, E.A., Erhardt, E.B., Calhoun, V.D., 2012a. Data visualization in the neurosciences: overcoming the curse of dimensionality. *Neuron* 74, 603–608.

Allen, E.A., Erhardt, E.B., Wei, Y.H., Eichele, T., Calhoun, V.D., 2012b. Capturing inter-subject variability with group independent component analysis of fMRI data: a simulation study. *Neuroimage* 59, 4141–4159.

Andreasen, N.C., Flaum, M., Swayze, V.d., O’Leary, D.S., Alliger, R., Cohen, G., Ehrhardt, J., Yuh, W.T., 1993. Intelligence and brain structure in normal individuals. *Am. J. Psychiatry* 150, 130–130.

Barbey, A.K., Colom, R., Solomon, J., Krueger, F., Forbes, C., Grafman, J., 2012. An integrative architecture for general intelligence and executive function revealed by lesion mapping. *Brain* 135, 1154–1164.

Bell, A.J., Sejnowski, T.J., 1995. An information maximization approach to blind separation and blind deconvolution. *Neural Comput.* 7, 1129–1159.

Biswal, B., Yetkin, F.Z., Houghton, V.M., Hyde, J.S., 1995. Functional connectivity in the motor cortex of resting human brain using echo-planar MRI. *Magn. Reson. Med.* 34, 537–541.

Bockholt, H.J., Scully, M., Courtney, W., Rachakonda, S., Scott, A., Caprihan, A., Fries, J., Kalyanam, R., Segall, J.M., de la Garza, R., Lane, S., Calhoun, V.D., 2010. Mining the mind research network: a novel framework for exploring large scale, heterogeneous translational neuroscience research data sources. *Front. Neuroinform.* 3, 36.

Bressler, S.L., Menon, V., 2010. Large-scale brain networks in cognition: emerging methods and principles. *Trends Cogn. Sci.* 14, 277–290.

Calhoun, V.D., Kiehl, K.A., Pearlson, G.D., 2008. Modulation of temporally coherent brain networks estimated using ICA at rest and during cognitive tasks. *Hum. Brain Mapp.* 29, 828–838.

Colom, R., Haier, R.J., Head, K., Alvarez-Linera, J., Quiroga, M.A., Shih, P.C., Jung, R.E., 2011. Gray matter correlates of fluid, crystallized, and spatial intelligence: testing the P-FIT model. *Intelligence* 37, 124–135.

Cordes, D., Houghton, V.M., Arfanakis, K., Wendt, G.J., Turski, P.A., Moritz, C.H., Quigley, M.A., Meyerand, M.E., 2000. Mapping functionally related regions of brain with functional connectivity MR imaging. *Am. J. Neuroradiol.* 21, 1636–1644.

Deary, I.J., 2012. Intelligence. *Annu. Rev. Psychol.* 63 (63), 453–482.

Deary, I.J., Penke, L., Johnson, W., 2010. The neuroscience of human intelligence differences. *Nat. Rev. Neurosci.* 11, 201–211.

Duncan, J., Owen, A.M., 2000. Common regions of the human frontal lobe recruited by diverse cognitive demands. *Trends Neurosci.* 23, 475–483.

Duncan, J., Seitz, R.J., Kolodny, J., Bor, D., Herzog, H., Ahmed, A., Newell, F.N., Emslie, H., 2000. A neural basis for general intelligence. *Science* 289, 457–460.

Garrity, A.G., Pearlson, G.D., McKiernan, K., Lloyd, D., Kiehl, K.A., Calhoun, V.D., 2007. Aberrant “default mode” functional connectivity in schizophrenia. *Am. J. Psychiatry* 164, 450–457.

Gläscher, J., Rudrauf, D., Colom, R., Paul, L.K., Tranel, D., Damasio, H., Adolphs, R., 2010. Distributed neural system for general intelligence revealed by lesion mapping. *Proc. Natl. Acad. Sci.* 107, 4705–4709.

Gray, J.R., Chabris, C.F., Braver, T.S., 2003. Neural mechanisms of general fluid intelligence. *Nat. Neurosci.* 6, 316–322.

Haier, R.J., Siegel Jr., B.V., Nuechterlein, K.H., Hazlett, E., Wu, J.C., Paek, J., Browning, H.L., Buchsbaum, M.S., 1988. Cortical glucose metabolic rate correlates of abstract reasoning and attention studied with positron emission tomography. *Intelligence* 12, 199–217.

Hassabis, D., Kumaran, D., Maguire, E.A., 2007. Using imagination to understand the neural basis of episodic memory. *J. Neurosci.* 27, 14365–14374.

Jafri, M.J., Pearlson, G.D., Stevens, M., Calhoun, V.D., 2008. A method for functional network connectivity among spatially independent resting-state components in schizophrenia. *Neuroimage* 39, 1666–1681.

Jung, R.E., Haier, R.J., 2007. The Parieto-Frontal Integration Theory (P-FIT) of intelligence: converging neuroimaging evidence. *Behav. Brain Sci.* 30, 135–154.

Kroger, J.K., Sabb, F.W., Fales, C.L., Bookheimer, S.Y., Cohen, M.S., Holyoak, K.J., 2002. Recruitment of anterior dorsolateral prefrontal cortex in human reasoning: a parametric study of relational complexity. *Cereb. Cortex* 12, 477–485.

Langer, N., Pedroni, A., Gianotti, L.R., Hanggi, J., Knoch, D., Jancke, L., 2012. Functional brain network efficiency predicts intelligence. *Hum. Brain Mapp.* 33, 1393–1406.

Langeslag, S.J.E., Schmidt, M., Ghassabian, A., Jaddoe, V.V.W., Hofman, A., van der Lugt, A., Verhulst, F.C., Tiemeier, H., White, T.J.H., 2013. Functional connectivity between parietal and frontal brain regions and intelligence in young children: the Generation R study. *Hum. Brain Mapp.* 34, 3299–3307.

Li, Y., Liu, Y., Li, J., Qin, W., Li, K., Yu, C., Jiang, T., 2009. Brain anatomical network and intelligence. *PLoS Comput. Biol.* 5, e1000395.

Luders, E., Narr, K.L., Thompson, P.M., Toga, A.W., 2009. Neuroanatomical correlates of intelligence. *Intelligence* 37, 156–163.

Paulus, M.P., Feinstein, J.S., Leland, D., Simmons, A.N., 2005. Superior temporal gyrus and insula provide response and outcome-dependent information during assessment and action selection in a decision-making situation. *Neuroimage* 25, 607–615.

Prabhakaran, V., Smith, J.A., Desmond, J.E., Glover, G.H., Gabrieli, J.D., 1997. Neural substrates of fluid reasoning: an fMRI study of neocortical activation during performance of the Raven’s Progressive Matrices Test. *Cogn. Psychol.* 33, 43–63.

Raven, J., 1990. *Advanced Progressive Matrices: Sets I and II*. Oxford Univ Press, Oxford.

Raven, J., 2000. The Raven’s progressive matrices: change and stability over culture and time. *Cogn. Psychol.* 41, 1–48.

Scott, A., Courtney, W., Wood, D., de la Garza, R., Lane, S., King, M., Wang, R., Roberts, J., Turner, J.A., Calhoun, V.D., 2011. COINS: an innovative informatics and neuroimaging tool suite built for large heterogeneous datasets. *Front. Neuroinform.* 5, 33.

- 474 Smith, S.M., Fox, P.T., Miller, K.L., Glahn, D.C., Fox, P.M., Mackay, C.E., Filippini, N.,  
475 Watkins, K.E., Toro, R., Laird, A.R., 2009. Correspondence of the brain's  
476 functional architecture during activation and rest. *Proc. Natl. Acad. Sci.* 106,  
477 13040–13045.
- 478 Snow, R., Kyllonen, C., Marshalek, B., 1984. The topography of ability and learning  
479 correlations. *Advances in the Psychology of Human Intelligence*. Erlbaum, Hillsdale,  
480 NJ, pp. 47–103.
- Song, M., Zhou, Y., Li, J., Liu, Y., Tian, L.X., Yu, C.S., Jiang, T.Z., 2008. Brain spontaneous 481  
functional connectivity and intelligence. *NeuroImage* 41, 1168–1176. 482
- Vakhtin, A.A., Calhoun, V.D., Jung, R.E., Prestopnik, J.L., Taylor, P.A., Ford, C.C., 2013. 483  
Changes in intrinsic functional brain networks following blast-induced mild 484  
traumatic brain injury. *Brain Inj.* 27, 1304–1310.
- van den Heuvel, M.P., Stam, C.J., Kahn, R.S., Pol, H.E.H., 2009. Efficiency of functional brain  
networks and intellectual performance. *J. Neurosci.* 29, 7619–7624.

UNCORRECTED PROOF